PDMS MICROSTRUCTURES 3D-NANOPRINTED INSIDE UNCOATED, ENCLOSED PDMS-ON-GLASS MICROCHANNELS *VIA IN SITU* DIRECT LASER WRITING

Xin Xu, Olivia M. Young, Adira Colton, and Ryan D. Sochol
University of Maryland, College Park, MD, USA

ABSTRACT

Polydimethylsiloxane (PDMS) is one of the most commonly used materials for soft lithography protocols and microfluidics research. Yet, for emerging applications that rely on "*in situ* Direct Laser Writing (*is*DLW)"—approaches in which microstructures are additively manufactured directly inside of enclosed microfluidic channels—PDMS has presented a number of challenges as a microchannel material, primarily stemming from difficulties in facilitating sufficient adhesion between printed structures and the channel wall. To address such issues and enable the facile fabrication of PDMS-based *is*DLW-printed microfluidic technologies, here we introduce a novel strategy for printing PDMS microstructures directly onto and fluidically sealed to uncoated PDMS sidewalls of enclosed PDMS-on-glass microfluidic channels. We investigated microchannel geometry (*e.g.*, rectangular, trapezoidal, and semi-ovular cross sections) as a determinant in microfluidic print-to-wall sealing efficacy for 10 μm-thick fluidic barrier microstructures printed in channels with heights and widths of 50 μm. Microfluidic burst-pressure results revealed that semi-ovular channels yielded superior sealing integrity with pressure tolerances up to 350 kPa (*i.e.*, >5× that of our prior work), suggesting that the presented strategy offers unique promise to enable new classes of PDMS-based 3D microfluidic structures for biomedical and soft robotic applications.

KEYWORDS

Additive Manufacturing, 3D Printing, Direct Laser Writing, Two-Photon Polymerization, Polydimethylsiloxane, Microfluidics

INTRODUCTION

Among current additive manufacturing (or "3D printing") technologies, "Two-Photon Direct Laser Writing (DLW)" is offers unparalleled geometric control and print speeds for fabricating structures with feature resolutions on the order of 100 nm [1-3]. One limitation in the use of DLW for manufacturing microfluidic systems is that this submicron resolution can also represent a burden for fabricating the macro-to-micro interfaces (*e.g.*, inlet and outlet ports) required for fluidic loading, control, and retrieval [4,5]. One prominent approach to circumvent this issue is the concept of "*in situ* DLW (*is*DLW)", which entails 3D printing microstructures directly inside of enclosed microfluidic channels [6,7]. For manufacturing enclosed microfluidic channels, researchers have often turned to polydimethylsiloxane (PDMS)—a biocompatible silicone elastomer that, due in part to its advantages in soft lithography protocols, is widely employed across biomedical, microfluidics, and soft robotics fields [8-10]. Unfortunately, PDMS has proven to be a particularly challenging material for use in *is*DLW approaches for which the printed microstructures must fully adhere to the microchannel walls (to prevent fluidic leakage) [11-15].

Researchers have explored a number of strategies to mitigate these PDMS-based adhesion issues. For example, researchers have tried infusing silane-based glues after the *is*DLW printing process [16]. Previously, our group introduced the concept of using sol-gel surface coatings to enhance print-to-wall adhesion [5]—an approach other groups have recently adapted [17]. Such surface coatings, however, rely on time, labor, and/or cost-intensive protocols [5,17]. Thus, new manufacturing methodologies are needed to enable *is*DLW within uncoated, enclosed PDMS-based microfluidic devices.

CONCEPT

To address the aforementioned challenges associated with executing *is*DLW protocols with PDMS-based microfluidic devices, here we introduce a novel *is*DLW strategy that leverages a PDMS-based, DLW-compatible photomaterial to allow for PDMS microstructures to be printed directly onto untreated PDMS channels inside of enclosed PDMS-on-glass microfluidic devices (**Fig. 1**). Our approach involves three key steps. First, DLW is used to print a microchannel mold, which is then replicated with PDMS using established protocols [5]. After bonding the replicated PDMS to a glass slide, the second step involves the passive vacuum loading [18] of the liquid-phase, low-viscosity photomaterial, IP-PDMS (Nanoscribe GmbH, Karlsruhe, Germany), into the PDMS-of-glass microchannels (**Fig. 1a**). Lastly, the microdevice is loaded into the DLW 3D printer for *is*DLW printing of the microfluidic barrier directly inside of (and sealed to) the uncoated PDMS channels *via* a "ceiling-to-floor" photopolymerization process (**Fig. 1b**).

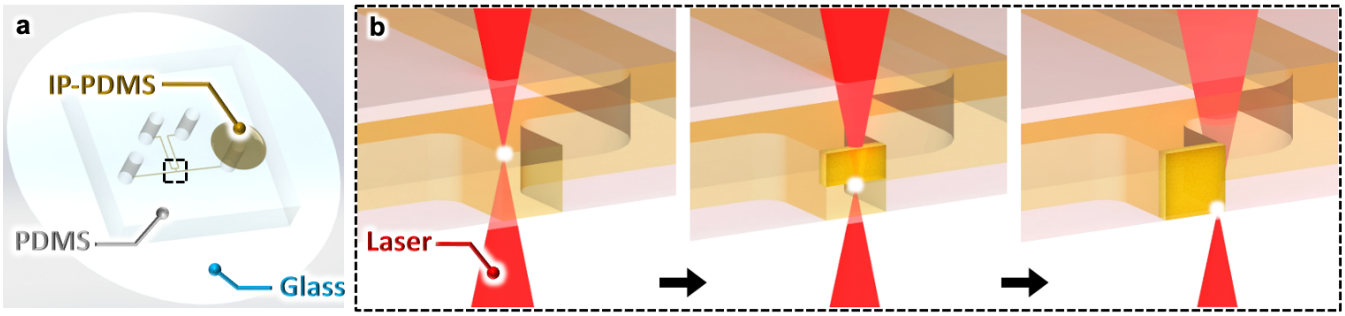

***Figure 1**: Concept of "in situ Direct Laser Writing (isDLW)" of polydimethylsiloxane (PDMS)-based microstructures directly inside of—and notably, fluidically sealed to—uncoated, enclosed PDMS-on-glass microfluidic channels. **(a)** Passive vacuum loading of the liquid-phase, low-viscosity photocurable material, IP-PDMS, into enclosed PDMS-on-glass microchannels. **(b)** The "ceiling-to-floor" isDLW process. A pulsed IR laser passes through an objective lens, immersion oil, glass substrate, and liquid-phase photomaterial to initiate spatially controlled photopolymerization (white) in a point-by-point, layer-by-layer methodology, ultimately producing a microstructure comprising cured PDMS-based photomaterial that is fully sealed to the entire luminal surface of the uncoated PDMS-on-glass channel.*

978-1-940470-04-7/HH2022/$25©2022TRF
DOI 10.31438/trf.hh2022.60

MATERIALS AND METHODS

"Direct Laser Writing (DLW)"-Based PDMS-on-Glass Microfluidic Device Fabrication

The PDMS-on-glass devices were fabricated as described previously [5]. Briefly, microchannel negative master molds were designed using the commercial computer-aided design (CAD) software, SolidWorks (Dassault Systèmes, France), and converted to the STL file format. All microchannels were designed with heights and widths of 50 μm; however, three distinct cross-sectional geometries were designed corresponding to rectangular, trapezoidal, and semi-ovular channel profiles. The STL files were then imported into the computer-aided manufacturing (CAM) software, Describe (Nanoscribe), to generate the laser writing path code for the DLW process. For the mold fabrication protocol, the slicing thickness and hatching parameters were set at 2.5 μm and 500 nm, respectively. Prior to the printing process, Si substrates (25 mm × 25 mm) were rinsed successively with acetone and isopropyl alcohol (IPA), and then dried with N_2 gas. The commercial photoresist, IP-Q (Nanoscribe), was deposited onto the Si substrates, which were then loaded into the Nanoscribe Photonic Professional GT2 DLW 3D printer using the 10× objective lens and Dip-in Laser Lithography (DiLL) configurations. After the DLW process, the substrates with printed patterns were developed in propylene glycol methyl ether acetate (PGMEA) for 25 min and IPA for 5 min to remove uncured residual photoresist. Developed molds were placed into a plastic petri dish, and a mixture of PDMS (Sylgard 184, Dow Corning, Corning, NY) prepared at a 10:1 (base to curing agent) ratio was then poured over the master molds, degassed, and placed on a hot plate set at 60 °C for 3 hours. Cured PDMS was then manually peeled off from the molds and punched with 0.75 mm inlet and outlet ports. The PDMS was rinsed with IPA and water, and then transferred to an O_2 plasma cleaner for bonding with 30 mm circular borosilicate glass substrates (#1.5, Bioptechs Inc., Butler, PA).

"*In Situ* DLW (*is*DLW)"-Based Fluidic Barrier Microstructure Fabrication

The fluidic barrier wall microstructures were modeled using SolidWorks (Dassault Systèmes) CAD software and designed with 10 μm overlap (with the PDMS microchannel and glass substrate) to promote fluidic sealing. The 3D CAD models of barrier designs corresponding to each channel profile were exported as STL files and then imported into Describe (Nanoscribe) CAM software for generation of the laser writing path code. The commercially available photoresist, IP-PDMS (Nanoscribe), was vacuum-loaded into the uncoated PDMS-on-glass microfluidic channels *via* the ports as described previously [18]. A droplet of immersion oil was placed on the underside of the glass substrate of the IP-PDMS-infused microdevice, which was then loaded into the Nanoscribe Photonic Professional GT2 DLW 3D printer with the 10× objective lens and oil-immersion mode configuration. For *is*DLW printing using IP-PDMS, the slicing thickness and hatching parameters were both set to 300 nm. The fluidic barrier microstructures were *is*DLW-printed by crosslinking the IP-PDMS in a point-by-point, layer-by-layer, "ceiling-to-floor" manner (*i.e.*, initially printing at the top of the PDMS microchannel and then ending the print at the glass substrate). Upon completion of the *is*DLW process, the microfluidic device was placed into an IPA solution for 20 min and then infused with fresh IPA through the microchannels to remove any residual photoresist. The device was then dried with N_2 gas.

Optical Characterization

Micrographs captured during the *is*DLW printing process of the barrier microstructures were carried out using the built-in Carl Zeiss Axio Observer inverted microscope (Zeiss, Germany) within the Nanoscribe Photonic Professional GT2 DLW 3D printer. Scanning electron microscopy (SEM) images were obtained using a TM4000 Tabletop SEM (Hitachi, Tokyo, Japan). To facilitate SEM imaging and characterizations of the *is*DLW-based prints, microchannels were first DLW-printed and molded to PDMS without bonding to glass substrates, and then the barrier microstructures (designed to have a slightly smaller height to prevent over-printing in which barrier walls exceed the height of microchannels) were printed in designated positions. Substrates and devices were rinsed with IPA and dried with N_2 gas prior to SEM imaging.

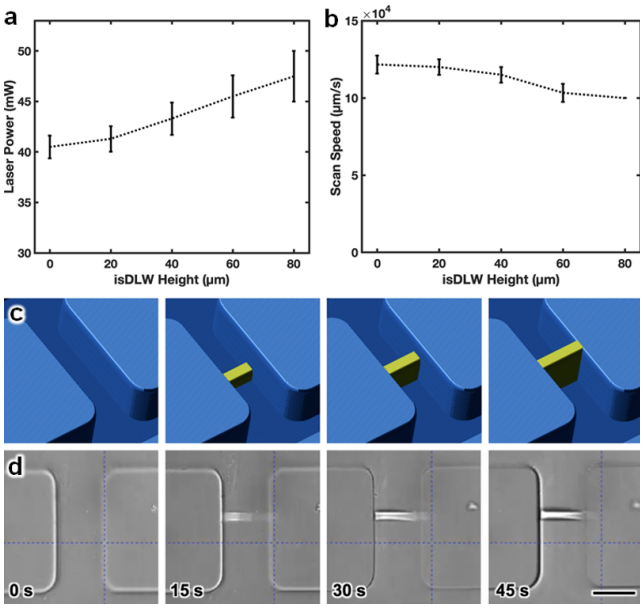

***Figure 2**: Fabrication results. **(a,b)** DLW print parameters associated with successful isDLW prints with respect to in-channel height. **(a)** Laser power. **(b)** Laser scan speed. Error bars = S.D.; n = 5. **(c, d)** Sequential computer-aided manufacturing (CAM) simulations **(c)** and corresponding micrographs **(d)** of the isDLW printing process for a barrier microstructure. Scale bar = 50 μm.*

Microfluidic Burst-Pressure Experimentation

Linear microfluidic burst-pressure experiments were performed using the Fluigent Microfluidic Control System (MFCS) and Flow Rate Platform and OxyGen software (Fluigent, France). This configuration allowed for simultaneous input pressure regulation and real-time monitoring and acquisition of both the pressure and flow rate data. To facilitate testing, microfluidic devices with *is*DLW-printed barrier microstructures were connected to fluorinate ethylene propylene fluidic tubing (Cole-Parmer, Vernon Hills, IL) *via* stainless-steel catheter couplers (20 ga., Instech, Plymouth Meeting, PA). Stainless steel catheter plugs (Instech) were inserted into superfluous ports. Burst pressure experiments were performed by applying an input pressure on one side of an *is*DLW-printed barrier microstructure, while fluid flow rates were recorded on the opposing side of the barrier structures. The input pressure was gradually increased at a rate of 2 kPa/s until the onset of leakage or burst events (*i.e.*, marked increases in the flow rate). Three experiments corresponding to each microchannel cross-sectional geometry (*i.e.*, rectangular, trapezoidal, and semi-ovular channel profiles) were performed. Data from all experiments were recorded in excel format and then processed using MATLAB (MathWorks, Natick, MA) to quantify the means and standard deviation (*S.D.*) of the pressure-flow rate relationships.

RESULTS AND DISCUSSIONS

PDMS-based *is*DLW Fabrication

To investigate the manufacturing efficacy of the *is*DLW strategy for printing microstructures inside of (and sealed to) enclosed, PDMS-on-glass microchannels that do not require pre-processing, such as surface coatings and chemical treatments [5,17], we explored the role of microchannel geometry in microfluidic sealing integrity. Using previously reported DLW-based micromolding protocols [5], we manufactured enclosed PDMS-on-glass microfluidic devices with a target region where the cross-sectional geometry of the 50 μm-tall microchannel was designed with either a rectangular, trapezoidal, or semi-ovular profile. We initially performed experiments to elucidate the DLW print settings that ensure appropriate exposure dosage at each height—*i.e.*, high enough to initiate photopolymerization, yet not too high to cause photomaterial burning issues. Fabrication results revealed that the effective laser power increased from 40.5±2.2 mW to 47.5±5.0 mW with height increasing from 0 to 80 μm, respectively (**Fig. 2a**), while the effective scan speed decreased from approximately 120 mm/s to 100 mm/s with height increasing from 0 to 80 μm, respectively (**Fig. 2b**). For consistency with prior reports for testing *is*DLW approaches [5,15,17], we examined manufacturing and microfluidic sealing efficacy using 10 μm-thick microfluidic barrier wall microstructures. CAM simulations and corresponding micrographs of the *is*DLW printing process are presented in **Figure 2c** and **2d**, respectively, with a total print time of approximately 45 s for each barrier structure.

SEM micrographs of the DLW-printed master molds, replicated PDMS microchannel cross sections, and *is*DLW-printed fluidic barrier microstructures within PDMS microchannels with the distinct channel geometries are presented in **Figure 3**. Fabrication results revealed that for 50 μm-tall channels, the printed barrier microstructures did not fully adhere to the sidewalls for the rectangular case (**Fig. 3a**); however, we did not observe such print-to-sidewall detachments for either the trapezoidal case (**Fig. 3b**) or the semi-ovular case (**Fig. 3c**). These fabrication results suggest that microchannels with effectively tapered sidewalls promote adhesion of *is*DLW-printed microstructures to the channel sidewalls, which is consistent with *is*DLW results from our prior studies [5,19].

Microfluidic Burst-Pressure Experimentation

To quantify the fluidic sealing integrity of the IP-PDMS barrier microstructures-to-PDMS microchannel interfaces, we performed linear microfluidic burst-pressure experiments for the distinct channel geometries (*i.e.*, rectangular, trapezoidal, and semi-ovular).

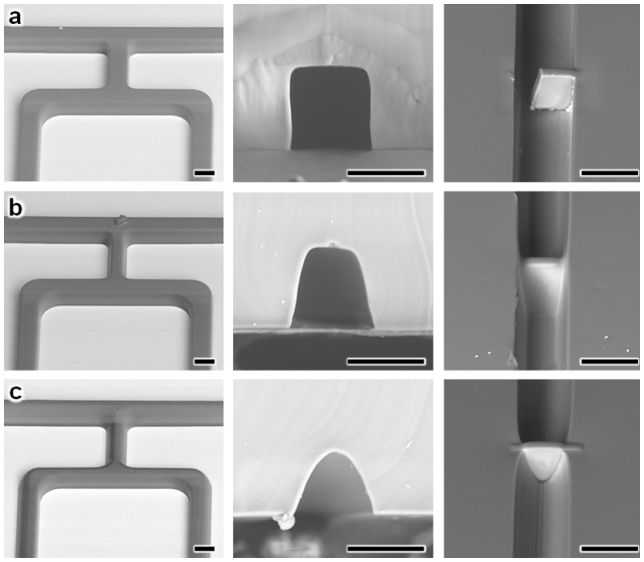

***Figure 3**: SEM micrographs of results for (left) DLW-printed master molds, (middle) replicated microchannel cross sections, and (right) barrier microstructures isDLW-printed in the micro-channels with **(a)** rectangular, **(b)** trapezoidal, and **(c)** semi-ovular cross-sectional geometries. Scale bars = 50 μm.*

The experimental results revealed that microchannel geometry can significantly affect the fluidic sealing efficacy of the *is*DLW-printed barrier structures (**Fig. 4**). Specifically, results for the rectangular channel profile revealed an onset of burst/leakage phenomena—indicated by abrupt increases in flow rate due to partial or full detachment of the barrier structure from the interior microchannel surfaces—at pressures below 200 kPa (**Fig. 4a**). The results for the trapezoidal channel profile revealed slightly higher burst pressures above 200 kPa (**Fig. 4b**). In contrast, the semi-ovular channel yielded the highest burst pressures of those examined in the current study, with fluidic sealing integrity maintained in excess of 350 kPa input pressures (**Fig. 4c**). These results for the semi-ovular channel geometry represent a >5× improvement *versus* our prior results for sol-gel-coated PDMS-on-glass microchannels [5]. Notably, even the results for the rectangular microchannel cross section—which exhibited the worst performance of the channel profiles investigated here—demonstrate significantly improved performance over the results reported in our prior work [5].

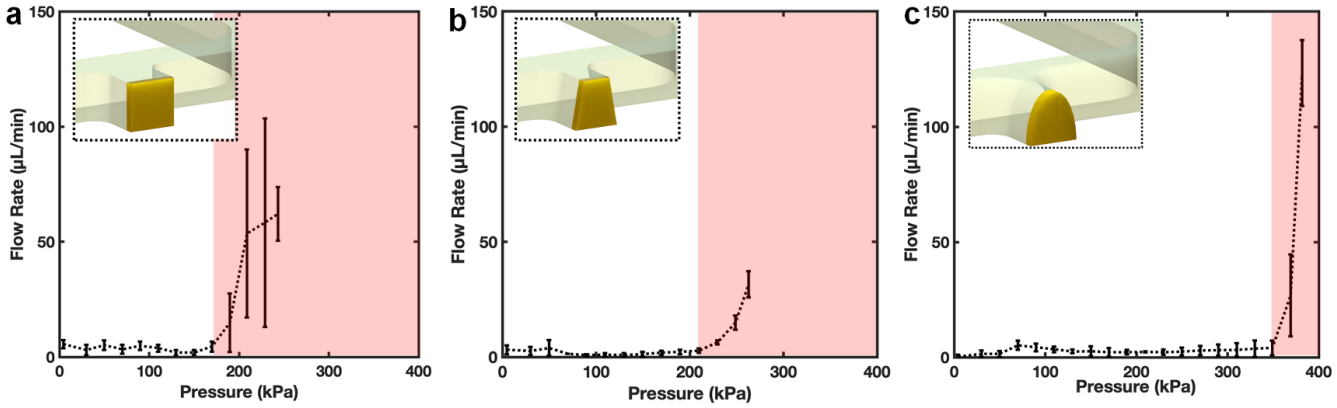

***Figure 4**: Quantified results for burst-pressure experiments with IP-PDMS barrier microstructures isDLW-printed inside of PDMS-on-glass microchannels corresponding to distinct cross-sectional profiles: **(a)** rectangular, **(b)** trapezoidal, and **(c)** semi-ovular. Red shaded regions denote undesired burst/leakage phenomena. Error bars = S.D.; n = 3 experiments per microchannel design.*

CONCLUSIONS

Recent advancements in the field of additive manufacturing provide significant promise for creating new classes of microfluidic systems that can, in turn, enable wide-ranging biomedical and soft robotic applications. In this work, we report the first demonstration of PDMS-based microstructures additively manufactured directly inside of—and notably, fluidically sealed to—uncoated, enclosed PDMS-on-glass microfluidic channels. The PDMS-based *is*DLW strategy and results presented in this work provide a preliminary foundation and guidelines for microstructure fabrication in PDMS without any pre-coating steps or post-printing infusions of glues. Akin to our prior studies [5,19], the fabrication and microfluidic burst-pressure testing results revealed that the microchannel cross-sectional geometry plays a critical role in the print-to-channel adhesion efficacy of the *is*DLW approach. In particular, we observed that 10 μm-thick barrier walls printed in 50 μm-tall microchannels with semi-ovular profiles nearly doubled the fluidic burst-pressure performance compared to that associated with the rectangular microchannel profiles. These results suggest that DLW-enabled microchannel geometries are preferable to standard rectangular profiles associated with conventional photolithography. Despite the relatively poor performance for the rectangular profile case, it should be noted that those results still represent a marked increase over our prior results that relied on time- and labor-intensive protocols for sol-gel coating of the PDMS channels [5]. One limitation of the current study is that, while the barrier microstructures were additively manufactured, their geometry is essentially 2.5D. Thus, future efforts should focus on interrogating the efficacy of the presented approach for fully 3D microstructures. Nonetheless, the notable fluidic sealing integrity results demonstrated here suggest that the presented *is*DLW strategy for printing PDMS-based microstructures within uncoated PDMS-on-glass devices offers a promising new pathway to diverse applications that benefit from geometrically sophisticated PDMS structures and systems at unprecedented size scales.

ACKNOWLEDGEMENTS

We greatly appreciate the contributions of members of the Bioinspired Advanced Manufacturing (BAM) Laboratory and the technical staff of Terrapin Works at the University of Maryland, College Park.

REFERENCES

[1] A. E. Goodling, S. Nagelberg, B. Kaehr, C. H. Meredith, S. I. Cheon, A. P. Saunders, M. Kolle, and L. D. Zarzar, "Colouration by total internal reflection and interference at microscale concave interfaces," *Nature*, vol. 566, no. 7745, pp. 523–527 (2019).

[2] M. Hippler, E. Blasco, J. Qu, M. Tanaka, C. Barner-Kowollik, M. Wegener, and M. Bastmeyer, "Controlling the shape of 3D microstructures by temperature and light," *Nature Communications*, vol. 10, no. 1 (2019).

[3] D. Nishiguchi, I. S. Aranson, A. Snezhko, and A. Sokolov, "Engineering bacterial vortex lattice via direct laser lithography," *Nature Communications*, vol. 9, no. 1 (2018).

[4] E. Montinaro, M. Grisi, M. C. Letizia, L. Pethö, M. A. Gijs, R. Guidetti, J. Michler, J. Brugger, and G. Boero, "3D printed microchannels for sub-nL NMR spectroscopy," *PLOS ONE*, vol. 13, no. 5 (2018).

[5] A. C. Lamont, A. T. Alsharhan, and R. D. Sochol, "Geometric determinants of in-situ direct laser writing," *Scientific Reports*, vol. 9, no. 1 (2019).

[6] M. H. Olsen, G. M. Hjortø, M. Hansen, Ö. Met, I. M. Svane, and N. B. Larsen, "In-chip fabrication of free-form 3D constructs for directed cell migration analysis," *Lab on a Chip*, vol. 13, no. 24, p. 4800 (2013).

[7] D. Wu, L.-G. Niu, S.-Z. Wu, J. Xu, K. Midorikawa, and K. Sugioka, "Ship-in-a-bottle femtosecond laser integration of optofluidic microlens arrays with center-pass units enabling coupling-free parallel cell counting with a 100% success rate," *Lab on a Chip*, vol. 15, no. 6, pp. 1515–1523 (2015).

[8] K. B. Justus, T. Hellebrekers, D. D. Lewis, A. Wood, C. Ingham, C. Majidi, P. R. LeDuc, and C. Tan, "A Biosensing Soft Robot: Autonomous parsing of chemical signals through integrated organic and inorganic interfaces," *Science Robotics*, vol. 4, no. 31 (2019).

[9] R. D. Sochol, A. T. Higa, R. R. Janairo, S. Li, and L. Lin, "Unidirectional mechanical cellular stimuli via micropost array gradients," *Soft Matter*, vol. 7, no. 10, p. 4606, (2011).

[10] R. Acevedo, M. A. Restaino, D. Yu, S. W. Hoag, S. Flank, and R. D. Sochol, "3D nanoprinted liquid-core-shell microparticles," *Journal of Microelectromechanical Systems*, vol. 29, no. 5, pp. 924–929 (2020).

[11] M. Restaino, N. Eckman, A. T. Alsharhan, A. C. Lamont, J. Anderson, D. Weinstein, A. Hall, and R. D. Sochol, "In situ direct laser writing of 3D graphene-laden microstructures," *Advanced Materials Technologies*, vol. 6, no. 8, p. 2100222 (2021).

[12] J. van 't Oever, N. Spannenburg, H. Offerhaus, D. van den Ende, J. L. Herek, and F. Mugele, "In-chip direct laser writing of a centimeter-scale acoustic micromixer," *Journal of Micro/Nanolithography, MEMS, and MOEMS*, vol. 14, no. 02, p. 1 (2015).

[13] L. Amato, Y. Gu, N. Bellini, S. M. Eaton, G. Cerullo, and R. Osellame, "Integrated three-dimensional filter separates nanoscale from microscale elements in a microfluidic chip," *Lab on a Chip*, vol. 12, no. 6, p. 1135 (2012).

[14] A.T. Alsharhan, O.M. Young, X. Xu, A.J. Stair, and R.D. Sochol, "Integrated 3D Printed Microfluidic Circuitry and Soft Microrobotic Actuators via *In Situ* Direct Laser Writing", *Journal of Micromechanics and Microengineering*, 31, 4 (2021).

[15] J. Y. Han, S. Warshawsky, and D. L. DeVoe, "In situ photografting during direct laser writing in thermoplastic microchannels," *Scientific Reports*, vol. 11, no. 1 (2021).

[16] J. Lölsberg, J. Linkhorst, A. Cinar, A. Jans, A. J. Kuehne, and M. Wessling, "3D nanofabrication inside rapid prototyped microfluidic channels showcased by wet-spinning of single micrometre fibres," *Lab on a Chip*, vol. 18, no. 9, pp. 1341–1348 (2018).

[17] A. Lüken, M. Geiger, L. Steinbeck, A. C. Joel, A. Lampert, J. Linkhorst, and M. Wessling, "Biocompatible micron-scale silk fibers fabricated by microfluidic wet spinning," *Advanced Healthcare Materials*, vol. 10, no. 20, p. 2100898 (2021).

[18] R. D. Sochol, S. Li, L. P. Lee, and L. Lin, "Continuous flow multi-stage microfluidic reactors via hydrodynamic microparticle railing," *Lab on a Chip*, vol. 12, no. 20, p. 4168 (2012).

[19] A. T. Alsharhan, R. Acevedo, R. Warren, and R. D. Sochol, "3D microfluidics *via* cyclic olefin polymer-based *in situ* direct laser writing," *Lab on a Chip*, vol. 19, no. 17, pp. 2799–2810 (2019).

CONTACT

Xin Xu, tel: +1-301-405-6928; xuxin97@umd.edu